Type Ic core-collapse supernova explosions evolved from very massive stars

Takashi Yoshida,[1]★ Shinpei Okita[2] and Hideyuki Umeda[2]

[1]*Yukawa Institute for Theoretical Physics, Kyoto University, Kyoto 606-8502, Japan*
[2]*Department of Astronomy, Graduate School of Science, University of Tokyo, Tokyo 113-0033, Japan*

ABSTRACT

We investigate the possibility of a superluminous Type Ic core-collapse supernovae (SNe) producing a large amount of ^{56}Ni. Very massive stars with a main-sequence mass larger than $100\,M_\odot$ and a metallicity $0.001 < Z \lesssim 0.004$ are expected to explode as superluminous Type Ic SNe. Stars with $\sim$110–150$\,M_\odot$ and $Z \lesssim 0.001$ would explode as Type Ic pulsational pair-instability SNe if the whole H and He layer has been lost by the mass-loss during pulsational pair instability. We evaluate the total ejecta mass and the yields of ^{56}Ni, O and Si in core-collapse SNe evolved from very massive stars. We adopt 43.1 and $61.1\,M_\odot$ WO stars with $Z = 0.004$ as SN progenitors expected to explode as Type Ic core-collapse SNe. These progenitors have masses of 110 and $250\,M_\odot$ at the zero-age main sequence. Spherical explosions with an explosion energy larger than 2×10^{52} erg produce more than $3.5\,M_\odot\,^{56}$Ni, enough to reproduce the light curve of SN 2007bi. Asphericity of the explosion affects the total ejecta mass as well as the yields of ^{56}Ni, O and Si. Aspherical explosions of the 110 and $250\,M_\odot$ models reproduce the ^{56}Ni yield of SN 2007bi. These explosions will also show large velocity dispersion. An aspherical core-collapse SN evolved from a very massive star is a possibility of the explosion of SN 2007bi.

Key words: nuclear reactions, nucleosynthesis, abundances – stars: evolution – supernovae: general – supernovae: individual: SN 2007bi – stars: Wolf–Rayet.

1 INTRODUCTION

Recent supernova (SN) surveys found a variety of superluminous SNe (SLSNe) in metal-poor galaxies (Quimby et al. 2011; Gal-Yam 2012). SLSNe indicate peak absolute magnitude less than $\sim$−21 mag and have a diversity of the rise and decline time in their light curves. SN 2007bi is a Type Ic SLSN (SLSNe Ic; Gal-Yam et al. 2009). Its light curve is well fitted to the radioactive decay of ^{56}Co, so that this explosion is considered to be powered by large amount of ^{56}Ni produced during the explosion of a very massive star (SLSN-R in Gal-Yam 2012). Since observational analyses indicated that the ^{56}Ni yield is 3.5–7.4 $M_\odot$, possibilities of pair-instability (PI) SN and core-collapse (CC) SN were proposed as the explosion mechanism (Gal-Yam et al. 2009; Moriya et al. 2010). The range of the main-sequence (MS) mass appropriate for SN 2007bi was evaluated as 525–575 $M_\odot$ for PI SN and 110–270 $M_\odot$ for CC SN explosions (Yoshida & Umeda 2011, hereafter abbreviated by YU11) in $Z = 0.004$ stars.

Asphericity of energetic CC explosion has been discussed as a comparison with the abundance patterns of extremely metal-poor (EMP) stars (e.g. Umeda & Nomoto 2002, 2005). Aspherical hypernovae well reproduced the abundance pattern of EMP stars (Tominaga 2009), so that hypernova explosion is expected to be aspherical. On the other hand, some energetic Type Ic SNe (SNe Ic) showed evidence for asphericity in late-time spectra (Maeda et al. 2008). The observational or indirect evidence of aspherical energetic CC explosions also suggests a possibility of aspherical CC explosion for SN 2007bi.

Recent observations revealed the existence of very massive stars. WN stars of 92–265 $M_\odot$ were found in the young star clusters NGC 3603 and R136 (Crowther et al. 2010). Their zero-age MS masses were evaluated up to 320 $M_\odot$. The evolution of very massive stars has been investigated and the final fates such as PI SNe and pulsational pair-instability (PPI) SNe were discussed (e.g. Langer et al. 2007; Waldman 2008; Yungelson et al. 2008; Chatzopoulos & Wheeler 2012a; Yusof et al. 2013). Recently, effects of eruptive mass-loss of very massive stars by PPI were also discussed (Woosley, Blinnikov & Heger 2007; Chatzopoulos & Wheeler 2012b). Although mass-loss rate of very massive stars is still uncertain, fates of very massive stars with current mass-loss rate should be investigated.

In this paper, we investigate the dependence of the final mass, the CO core mass and the stellar types on the MS mass with the

★ E-mail: yoshida@yukawa.kyoto-u.ac.jp

metallicity range $Z = 10^{-4}$–0.02. We discuss progenitors appropriate for CC SLSNe Ic. We also investigate the explosive nucleosynthesis of CC SNe evolved from very massive stars. We consider two different features of explosions: spherically symmetrical explosions with different explosion energies and 2D aspherical explosions with different opening angles of mass ejected region. We discuss the dependence of the total ejecta mass and the yields of ^{56}Ni, O and Si on explosion features.

In Section 2, we show the final mass and the CO core mass among stars with an MS mass $M_{\rm MS} = 13$–300 M$_\odot$ and a metallicity $Z = 10^{-4}$–0.02. We also show the progenitor models evolved from 110 and 250 M$_\odot$ stars with $Z = 0.004$ as progenitors of SLSNe Ic. In Section 3, we show the dependence of the yields of ^{56}Ni, O and Si on the explosion energy of spherically symmetrical CC SN explosions. In Section 4, we present the dependence on asphericity of aspherical CC SN explosions. Progenitors of SLSNe Ic, especially SN 2007bi, and aspherical CC SNe Ic evolved from very massive stars are discussed in Section 5. Conclusions are presented in Section 6.

2 VERY MASSIVE PROGENITORS

We calculate the evolution of massive stars until the central C-depletion with the ranges of an MS mass $M_{\rm MS} = 13$–300 M$_\odot$ and a metallicity $Z = 10^{-4}$–0.02 using the stellar evolution code in YU11 and Umeda, Yoshida & Takahashi (2012). The species of nuclei adopted in the nuclear reaction network is listed in Table 1. The mass-loss recipe taken in this study is the same as in Case (A) in YU11.

Fig. 1(a) shows the relation between the MS mass and the final mass of massive stars. In stars with $M_{\rm MS} \gtrsim 40$ M$_\odot$ and $Z \gtrsim 0.01$, strong mass-loss strips the whole H and/or He layers. These stars become Wolf–Rayet (WR) stars and their final masses become ∼10–30 M$_\odot$. Very massive stars with $M_{\rm MS} \gtrsim 100$ M$_\odot$ and $Z = 0.004$ become WO stars. Stars with $Z \lesssim 0.001$ possess the H and/or He layers until the C-burning. If the whole H and He layer is not lost by eruptive mass-loss induced by luminous blue variable-like events or PPI, these stars would explode as SNe II or Ib. We will discuss the effect by eruptive mass-loss during PPI later.

Table 1. Nuclear reaction network used for stellar evolution and explosive nucleosynthesis during SN explosion. Isomer of ^{26}Al is taken into account.

Element	A	Element	A
n	1	Ar	34–43
H	1–3	K	36–45
He	3–4	Ca	38–48
Li	6–7	Sc	40–49
Be	7, 9	Ti	42–51
B	8, 10, 11	V	44–53
C	11–13	Cr	46–55
N	13–15	Mn	48–57
O	14–18	Fe	50–61
F	17–19	Co	51–62
Ne	18–22	Ni	54–66
Na	21–23	Cu	56–68
Mg	22–27	Zn	59–71
Al	25–29	Ga	61–73
Si	26–32	Ge	63–75
P	27–34	As	65–76
S	30–37	Se	67–78
Cl	32–38	Br	69–79

Fig. 1(b) shows the relation between the CO core mass and the MS mass. The maximum mass of the CO core increases with decreasing the metallicity. Stars with $Z = 0.01$ and 0.004 have larger CO core than stars with the same MS mass and $Z = 0.02$ owing to smaller mass-loss rate. The mass range of CO core among WR stars depends on metallicity. The ranges are 8–11, 17–27 and 39–69 M$_\odot$ for WO stars with $Z = 0.02$, 0.01 and 0.004, respectively. Among stars with $Z = 0.001$ and 10^{-4}, metallicity dependence of the CO core mass is quite small.

We note that stars having a CO core of ∼40–60 M$_\odot$ experience PPI (Heger & Woosley 2002) and their outer layer is lost (Woosley et al. 2007). We expect that the stars in the region enclosed by the dashed line in Fig. 1(a) will become PPI. The ejected amount of the outer layer will strongly depend on pulsations of PPI and the density structure. If the whole H and He layer of stars with $M_{\rm MS} \sim 110$–150 M$_\odot$ and $Z \lesssim 0.001$ is lost by eruptive mass-loss during PPI, these stars will explode as SNe Ic.

In the following sections, we use progenitors to study SLSNe Ic evolved from very massive stars with MS masses $M_{\rm MS} = 110$ and 250 M$_\odot$ and a metallicity $Z = 0.004$. Since the metallicity of the host galaxy of SN 2007bi is $Z = 0.2$–0.4 Z$_\odot$ (Young et al. 2010), the metallicity of our progenitor models is within the range of the host galaxy of SN 2007bi. We calculated the evolution of these two models up to the onset of the CC, i.e. the central temperature of $\log T_{\rm C} \sim 9.8$. We added an acceleration term to the hydrostatic equation after the C-burning (e.g. Sugimoto, Nomoto & Eriguchi 1981). These models lose all H-rich envelope during He burning and almost all He layer after the central He burning and evolve to WO stars. The final mass $M_{\rm f}$, the CO core mass $M_{\rm CO}$, the Fe core mass $M_{\rm Fe}$, the surface He amount $M({\rm He})$ and the He mass fraction at the surface Y_S of these progenitors are listed in Table 2. The CO core is defined as the region where He mass fraction is smaller than 10^{-3} (Umeda & Nomoto 2008). The Fe core is defined as the region where the total mass fraction of the elements heavier than Sc is larger than 0.5 (Hirschi, Meynet & Maeder 2004). These stars are expected to explode as an SN Ic because of small He mass fraction at surface (e.g. Yoon, Woosley & Langer 2010). The $M_{\rm MS} = 250$ M$_\odot$ star experienced PPI during the Si burning (e.g. Umeda & Nomoto 2008). We do not consider eruptive mass-loss during PPI. The effect of the eruptive mass-loss will be discussed in Section 5.

3 SPHERICAL SUPERNOVA EXPLOSION

First, we investigate the explosive nucleosynthesis of spherical SN explosions. We calculate time evolution of 1D spherical SN explosion using a piecewise parabolic method code (Colella & Woodward 1984) as in Umeda & Nomoto (2005). Thermal energy is injected inside the mass cut to explode the star. We set the location of the mass cut to be 2.0 M$_\odot$. We consider eight explosion models of which explosion energies above the mass cut are $E_{\rm ex, 51} = 1, 5, 10, 20, 30, 50, 70$ and 100, where $E_{\rm ex, 51}$ is the explosion energy in units of 10^{51} erg. Then, we calculate the nucleosynthesis during the SN explosions by post-processing. The nuclear reaction network is the same as in the stellar evolution code. When the temperature is higher than 9×10^9 K, chemical composition is solved assuming nuclear statistical equilibrium. The ν-process is included with a parameter set independent of the explosion model as in Yoshida, Umeda & Nomoto (2008). The total neutrino energy is assumed to be 3×10^{53} erg. The neutrino luminosity decreases exponentially with time with a time-scale of 3 s. The neutrino spectra obey Fermi–Dirac distributions with zero chemical potentials. The temperatures are set to be 4.0 MeV for ν_e and $\bar{\nu}_e$, and 6.0 MeV for $\nu_{\mu, \tau}$ and
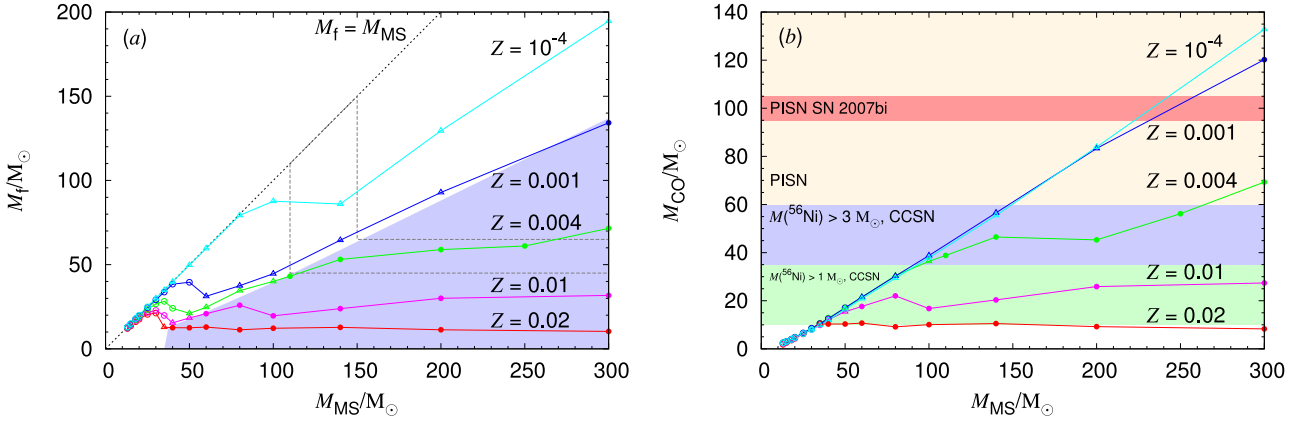
Figure 1. The relation of the final mass M_f (panel a) and the CO core mass M_{CO} (panel b) to the MS mass M_{MS} of stars with metallicities $Z = 0.02$ (red line), 0.01 (purple line), 0.004 (green line), 0.001 (blue line) and 10^{-4} (cyan line). The open circles, triangles and closed circles indicate red supergiants, yellow supergiants or WN stars and WO stars, respectively. In panel (a), progenitors in the blue shaded region are WO stars and are expected to explode as SNe Ic. The stars in the region enclosed by the dashed line will experience PPI (see the text for details). The dotted line shows $M_f = M_{MS}$. In panel (b), green and blue regions indicate the CC SN explosions ejecting ^{56}Ni more than 1 and 3 $M_\odot$, respectively. The orange region indicates PI SN. The red region is for the CO core mass range expected to reproduce the ^{56}Ni yield in SN 2007bi.

Table 2. Progenitors of SNe Ic.

$M_{MS}/M_\odot$	110	250
$M_f/M_\odot$	43.1	61.1
$M_{CO}/M_\odot$	38.2	56.2
$M_{Fe}/M_\odot$	3.03	3.21
$M(He)/M_\odot$	0.24	0.51
Y_S	0.191	0.193

$\bar{\nu}_{\mu,\tau}$. The rates of the ν-process reactions are adopted from Hoffman & Woosley (1992),[1] Horowitz (2002), Yoshida et al. (2008) and Suzuki et al. (2009). We note that although the ν-process has large uncertainties in SN explosions of very massive stars, it is not important for the production of ^{56}Ni, O and Si.

Fig. 2 shows ^{56}Ni and Si yields in the SN ejecta as a function of the explosion energy $E_{ex,51}$. The obtained ^{56}Ni yield will correspond to the maximum yield produced through aspherical explosion with the same explosion energy. The ^{56}Ni yield increases with the explosion energy and scarcely depends on the mass of the progenitor in the case of $E_{ex,51} \gtrsim 10$. The maximum ^{56}Ni yield is 6.8 and 6.4 $M_\odot$ in $E_{ex,51} = 100$ for the 110 and 250 $M_\odot$ models. The ^{56}Ni yield of more than 3.5 $M_\odot$, which reproduces the amount observed in SN 2007bi, is obtained from the explosions with $E_{ex,51} \gtrsim 20$. The Si yield of the 110 and 250 $M_\odot$ SN models are $M(Si) \sim 2.45$–3.65 and 5.38–$5.82 M_\odot$ in $E_{ex,51} \gtrsim 10$. The explosion-energy dependence is smaller than that of ^{56}Ni. As the explosion energy increases, the Si abundant region shifts outwards, but the width of the Si abundant region in the mass coordinate scarcely changes. The Si yield of the 250 $M_\odot$ model is larger than that in the 110 $M_\odot$ model. More Si is produced through the O shell burning during and after PPI in the 250 $M_\odot$ model.

We note that some materials fell back to the central remnant in the explosions with $E_{ex,51} = 1$ for the 110 $M_\odot$ model and with $E_{ex,51} = 1$ and 5 for the 250 $M_\odot$ model. In these three models, the baryon masses of the final remnants are 28.17, 46.56 and 7.32 $M_\odot$. Although about 2 $M_\odot$ of ^{56}Ni was synthesized during the
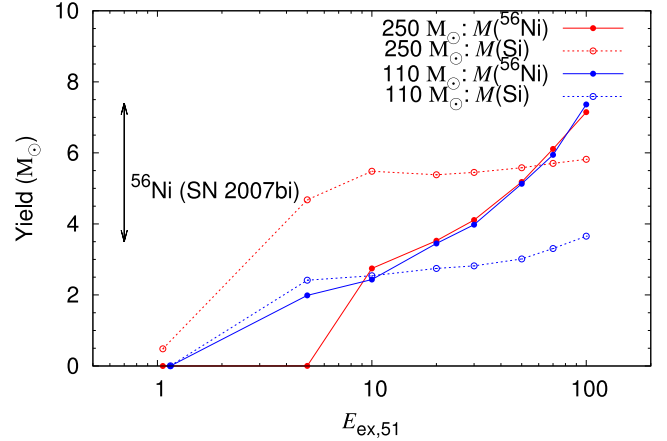
Figure 2. The yields of ^{56}Ni (solid line with closed circles) and Si (dotted line with open circles) ejected by spherical explosions of the 110 and 250 $M_\odot$ models as a function of the explosion energy $E_{ex,51}$. The red and blue lines indicate the yields of the 110 and 250 $M_\odot$ models, respectively. The observed range of the ^{56}Ni yield in SN 2007bi is indicated by the vertical arrow.

explosions, almost all ^{56}Ni fell back. Therefore, these explosions are not classified into SLSNe.

4 ASPHERICAL SUPERNOVA EXPLOSION

We calculate aspherical SN explosions with different opening angles using 2D Eulerian aspherical hydrodynamic code (Okita, Umeda & Yoshida 2012). We initially inject kinetic energy for 10^{-3} s in the innermost region of the ejecta to explode with a total explosion energy $E_{ex,51} = 50$ and 70 in the cases of the 110 $M_\odot$ model and the 250 $M_\odot$ model, respectively. These explosion energies in spherical explosions roughly reproduce the photometric velocity of SN 2007bi $\sim 12\,000$ km s^{-1} identified by Gal-Yam et al. (2009). We discuss ejecta velocities in aspherical explosions later. The injected kinetic energy is immediately converted into local thermal energy. We locate a central remnant of 2.0 $M_\odot$ corresponding to the mass cut for spherical explosion. An approximated analytical

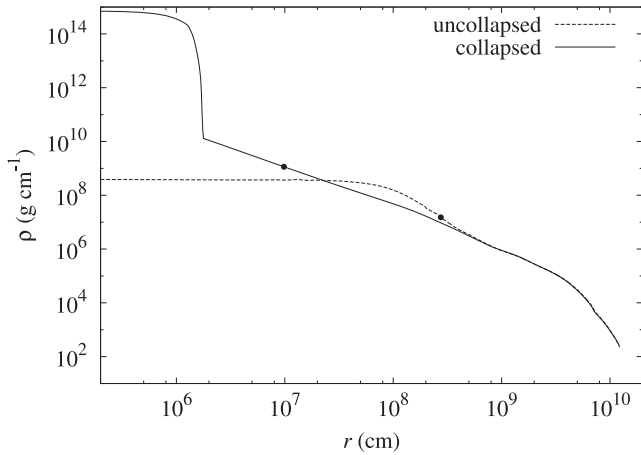**Figure 3.** Density distribution as a function of the radius for the uncollapsed (dashed line) and collapsed (solid line) progenitors of the $110 \, M_\odot$ model. The points indicate the location of the mass cut at $2.0 \, M_\odot$ in the mass coordinate.

equation of state including ultrarelativistic electrons and positrons at high temperature (e.g. Tominaga 2009) is adopted for the calculations;

$$P = \frac{kT}{\mu m_u} + \frac{aT^4}{3} \left(1 + \frac{7}{4} \frac{T_9^2}{T_9^2 + 5.3} \right), \tag{1}$$

where P is pressure, k is Boltzmann constant, T is temperature, μ is the mean molecular weight, which is assumed to be 2 here, m_u is the atomic mass unit, a is a radiation density constant and T_9 is temperature in units of 10^9 K. We choose several different opening angles θ_{op} of the polar ejected region. Then, we calculate the nucleosynthesis in the SN ejecta post-processingly using particle trace method. The orbits of 5200 Lagrangian particles are taken into account.

In this study, we adopt two density profiles for each progenitor as the initial conditions of the hydrodynamical calculations. The first one is the final density profile of the stellar evolution calculation. The other is the density profile obtained by the CC calculation. We pursued the CC until the mass of the collapsed matter corresponding to a proto-neutron star or a black hole becomes about $2 \, M_\odot$. During the CC, the radius at the mass coordinate of $2.0 \, M_\odot$ changed from 2.9×10^8 to 9.8×10^6 cm for the $110 \, M_\odot$ model and from 1.5×10^8 to 1.0×10^7 cm for the $250 \, M_\odot$ model. We call the former progenitor 'uncollapsed progenitor model' and the latter progenitor 'collapsed progenitor model'. Fig. 3 shows the density distribution of the uncollapsed and collapsed progenitors of the $110 \, M_\odot$ model. Since the central region of the progenitor should contract before aspherical explosion, we consider that collapsed progenitor model shows more realistic feature.

4.1 Aspherical explosions from uncollapsed progenitors

We first evaluate the yields of the aspherical SN explosions from the uncollapsed 110 and $250 \, M_\odot$ models. Fig. 4 shows the yields of ^{56}Ni, O and Si, and the total ejecta mass as a function of the opening angle. The ^{56}Ni yield ranges in $2.0–4.8 \, M_\odot$ for the $110 \, M_\odot$ model and $2.9–5.5 \, M_\odot$ for the $250 \, M_\odot$ model. The yield in small opening angle with $\theta_{op} \lesssim 45°$ for $110 \, M_\odot$ model is about 40 per cent of the yield for the spherical explosion. The aspherical explosion of the $250 \, M_\odot$ model with $\theta_{op} \lesssim 45°$ produces ^{56}Ni of about a half amount

compared with that produced in the spherical explosion. On the other hand, large opening angle case with $\theta_{op} \gtrsim 68°$ in the $250 \, M_\odot$ model indicates the ^{56}Ni yield similar to the yield obtained from the spherical explosion. The ^{56}Ni yield increases with the opening angle in $\theta_{op} \gtrsim 45°$ for the $110 \, M_\odot$ model and in $45° \lesssim \theta_{op} \lesssim 68°$ for the $250 \, M_\odot$ model. The dependence on the opening angle is mainly due to the difference in the efficiency of the fallback of the burned materials into the central remnant. The amount of ^{56}Ni produced during the explosion scarcely depends on the opening angle.

The opening-angle dependence of the ^{28}Si yield is similar to the ^{56}Ni yield. We see the increase with the opening angle in the ^{28}Si yield for slightly smaller opening angles than in the ^{56}Ni yield; $45° \lesssim \theta_{op} \lesssim 68°$ for the $110 \, M_\odot$ model and $11° \lesssim \theta_{op} \lesssim 68°$ for the $250 \, M_\odot$ model. This is mainly because Si is produced outside the ^{56}Ni-forming region. In larger opening angles, the fallback is suppressed in the Si-forming region. We see small dependence of the O yield on the opening angle. This is because most of the O is located in outer regions. A small amount of O in the equatorial region falls back and that in the polar region burns into Si and other intermediate nuclei in small opening angle cases.

The total ejecta mass increases with an opening angle. The lower limits of the ejecta mass are 28.4 and $47.5 \, M_\odot$. When the opening angle is small, the innermost materials fall back to the central remnant through the equatorial region. On the other hand, the explosion with a larger opening angle suppresses the fallback. The aspherical explosion induces upstream along the polar axis as well as fallback.

We note that we simplified the equation of state and did not consider the generation and absorption of nuclear energy with α-network in 2D explosion model. So, we briefly discuss differences between the abundance distributions calculated using 1D code and those using 2D code for spherical explosion models. The difference of the ^{56}Ni yield between 1D and 2D codes is less than 9 per cent. For the yields of C, O, Na, Mg, Si and Ca, which are listed in Table 3, the difference is less than 13 per cent for Na, 12 per cent for Ca and 7 per cent for the other elements. Thus, although the ^{56}Ni yield is slightly smaller in the result with the 2D code, we consider that difference in the adopting codes for solving the explosive nucleosynthesis does not give a large difference in the yields listed above.

4.2 Aspherical explosions from collapsed progenitors

Next, we evaluate the yields of the aspherical SN explosions from the collapsed progenitors. Fig. 5 shows the yields of ^{56}Ni, O, Si and the total ejecta amount relating to the opening angle of aspherical explosions with the collapsed 110 and $250 \, M_\odot$ models. The ^{56}Ni yield is in the range 3.7–5.9 and $4.8–6.1 \, M_\odot$ for the 110 and $250 \, M_\odot$ models, respectively. Although the yields and the total ejecta mass increase with the opening angle, the dependence is much smaller than that of the corresponding uncollapsed model. The yields of Si and O scarcely depend on the opening angle. These yields are also very close to the corresponding spherical explosion models from the uncollapsed progenitors.

The opening-angle dependence of the yields in the collapsed models is very small. The explosion of a small opening angle of a collapsed model indicated an explosion feature close to spherical symmetry compared with the corresponding explosion of the uncollapsed model. The final spacial distribution of the yields of the collapsed model of $\theta_{op} = 11°.25$ is close to the uncollapsed model of $\theta_{op} = 67°.5$. The ejecta mass also scarcely depends on the opening angle and is larger than that of the corresponding uncollapsed model. In the collapsed model, the energy-injection radius is
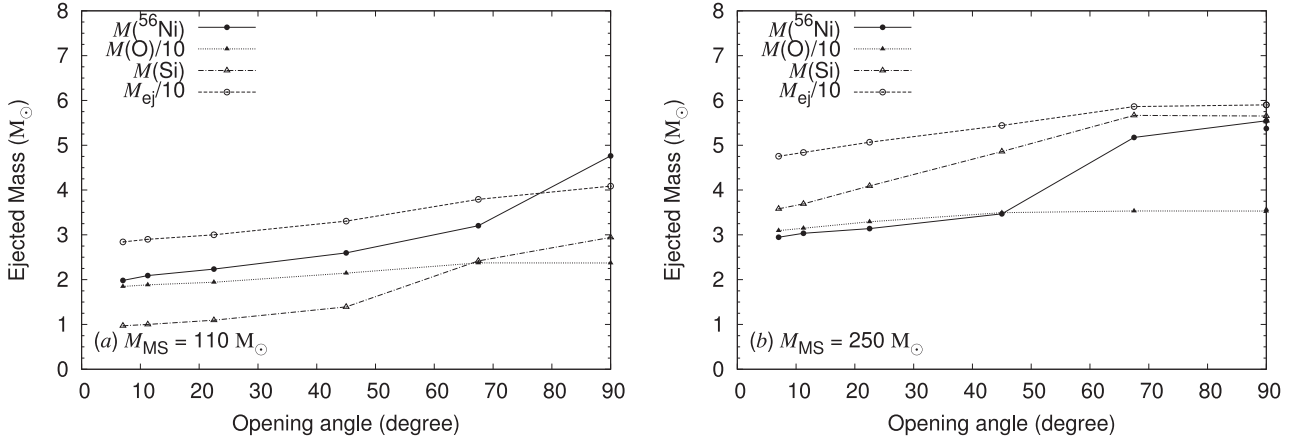
Figure 4. The yields of ^{56}Ni (solid line), O (dotted line) and Si (dash–dotted line), and the total ejecta amount M_{ejecta} (dashed line) in the aspherical explosion models of the uncollapsed progenitors. The MS mass M_{MS} and the explosion energy $E_{\text{ex, 51}}$ are set to be (a) 110 M$_\odot$ and 50, and (b) 250 M$_\odot$ and 70.

Table 3. The yields of spherical and aspherical CC SN models and PI SN models. In spherical CC SN models, M110E50 and M250E70 indicate the SN explosions of $(M_{\text{MS}}, E_{\text{ex, 51}}) = (110\,\text{M}_\odot, 50)$ and $(250\,\text{M}_\odot, 70)$, respectively. In aspherical CC SN models, M110θ_{op}11.25 and M250θ_{op}11.25 indicate the SN explosions of $(M_{\text{MS}}, E_{\text{ex, 51}}, \theta_{\text{op}}) = (110\,\text{M}_\odot, 50, 11°.25)$ and $(250\,\text{M}_\odot, 70, 11°.25)$, respectively. We adopted the results of the collapsed aspherical models. For PI SN models, MHe100 and M200 correspond to the PI SN models of $M_{\text{He}} = 100\,\text{M}_\odot$ He star in Heger & Woosley (2002) and $M = 200\,\text{M}_\odot$ metal-free star in Umeda & Nomoto (2002). SN 2007bi indicates the yield ranges of SN 2007bi obtained by six measurements listed in table 1 of Gal-Yam et al. (2009). For ^{56}Ni yield, the estimate from the observed peak luminosity is also taken into account.

| Element | Spherical CC SN models | | Aspherical CC SN models | | PI SN models | | SN 2007bi |
	M110E50	M250E70	M110θ_{op}11.25	M250θ_{op}11.25	MHe100 (HW02)	M200 (UN02)	
C	2.51	2.71	2.52	2.74	4.01	4.24	1.0–1.2
O	23.6	34.9	22.4	34.8	43.9	56.0	7.5–14.6
Na	0.008 00	0.008 31	0.007 68	0.008 52	0.002 76	0.007 00	0.0012–0.0023
Mg	1.10	1.53	1.01	1.56	4.41	3.08	0.065–0.13
Si	3.01	5.70	3.00	5.65	23.1	21.2	–
Ca	0.29	0.43	0.24	0.39	1.22	2.32	0.75–1.10
^{56}Ni	5.13	6.11	3.69	4.74	5.82	7.2	3.5–7.4
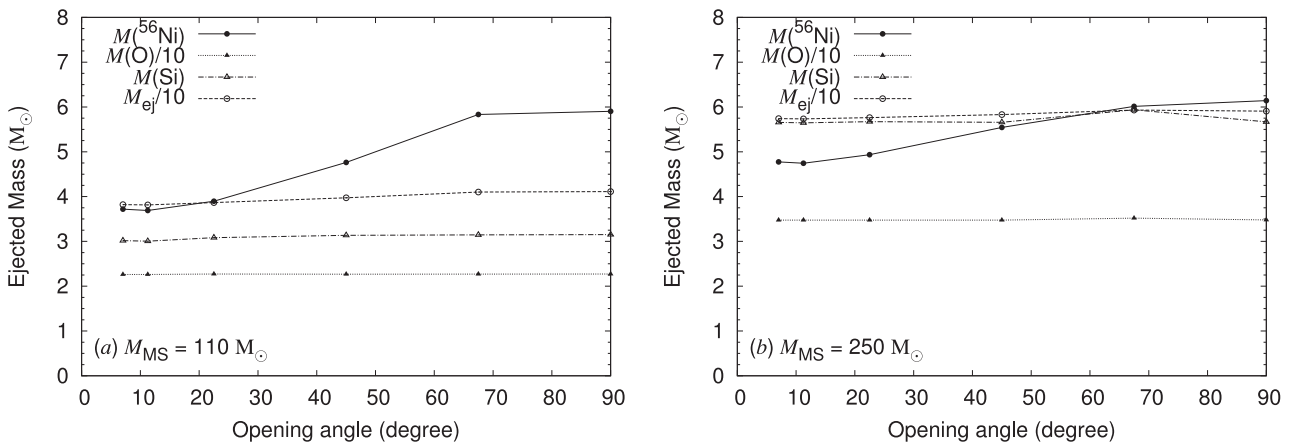
Figure 5. Same as Fig. 4, but for the aspherical explosion models of the collapsed progenitors.

smaller by about one order of magnitude than that of the uncollapsed model. The explosion becomes close to 'point-like' explosion even in ^{56}Ni-forming region. Thus, the dependence on the opening angle is smaller in the collapsed models.

We note that we set the energy deposition time to be 10^{-3} s in this study. However, energy deposition time of aspherical SNe is quite uncertain and will strongly affect the explosion feature and the yield distribution. Larger energy deposition time is expected to reduce the production and ejection of ^{56}Ni (e.g. Tominaga et al. 2007). The ^{56}Ni yield evaluated using the collapsed model would be the maximum value of the ^{56}Ni yield with a given explosion energy and an opening angle.

5 DISCUSSION

5.1 SL SN from very massive stars

Radioactive decay of ^{56}Ni and ^{56}Co is one of main light sources of SLSNe. Umeda & Nomoto (2008) showed that more than $1\,M_\odot$ ^{56}Ni is ejected by CC explosion when the CO core is roughly larger than $10\,M_\odot$ and the explosion energy is larger than $E_{ex,51} = 10$. A CO core larger than $\sim 35\,M_\odot$ with $E_{ex,51} \gtrsim 20$ will eject more than $3\,M_\odot$ ^{56}Ni (see also YU11). On the other hand, a progenitor with a CO core larger than $\sim 60\,M_\odot$ will explode as a PI SN. We draw the shaded regions satisfying the above conditions on the CO core masses in Fig. 1(b). Therefore, we expect that CC SNe Ic which eject more than $1\,M_\odot$ ^{56}Ni are possible for stars with $M_{MS} \gtrsim 30\,M_\odot$ and $Z > 0.004$. CC explosions evolved from very massive stars with $100 \lesssim M_{MS} \lesssim 250\,M_\odot$ and $0.001 < Z \lesssim 0.004$ would become SLSNe Ic similar to SN 2007bi. Stars with $M_{MS} \sim 110$–$150\,M_\odot$ and $Z \lesssim 0.001$ are expected to experience PPI and the whole H and He layer may be lost. In this case, these stars will also explode as SLSNe Ic.

Recently, Yusof et al. (2013) studied the evolution and fate of very massive stars. They evaluated the initial mass range of a PI SN progenitor for SN 2007bi as $M_{MS} = 160$–$170\,M_\odot$ based on their evolution calculations of 150–300 rotating stars with $Z = 0.002$. This mass is smaller than the one evaluated in YU11. One reason is the use of different mass-loss rate. The mass-loss rate in WR phase in our study seems to be larger than their rate. The metallicity dependence of our rate in MS stars [$\propto (Z/Z_\odot)^{0.64\text{–}0.69}$] is weaker than their rate [$\propto (Z/Z_\odot)^{0.85}$] and thus, our rate is practically larger. Another reason is larger CO-core mass in their models. The CO-core masses of their $M_{MS} = 150$–$200\,M_\odot$ models are larger than those of our models with $Z = 10^{-4}$, in which mass-loss does not affect the CO-core mass. This is probably due to rotation-induced mixing. Decrease in the lowest mass for PI SN by stellar rotation was shown in Chatzopoulos & Wheeler (2012a).

5.2 Yields of SN 2007bi

SN 2007bi is considered to eject ^{56}Ni of 3.5–$7.4\,M_\odot$. In order to explain the ^{56}Ni amount by spherical SN explosion of a 40–$60\,M_\odot$ CO star, the explosion energy should be $E_{ex,51} \gtrsim 20$. The explosion should be very energetic. This result is consistent with the estimate of the ejected ^{56}Ni amount in Umeda & Nomoto (2008). On the other hand, if the explosion energy is $E_{ex,51} \lesssim 5$, almost all ^{56}Ni falls back into the central remnant even if ^{56}Ni is produced explosively. In such a case, the exploded materials cannot be brightened by the radioactive decays of ^{56}Ni and ^{56}Co. Normal explosion of a very massive star will become a faint SN.

Here, we discuss a possibility of aspherical CC explosion of SN 2007bi. In the case of the collapsed progenitor models, which is expected to be more realistic, all aspherical explosions of the 110 and $250\,M_\odot$ models reproduce the ^{56}Ni yield of SN 2007bi. In the uncollapsed models, the range of the opening angle obtaining the ^{56}Ni mass more than $3.5\,M_\odot$ is $\theta_{op} \gtrsim 68°$ and $35°$ for the 110 and $250\,M_\odot$ models, respectively. Thus, aspherical explosions with a small opening angle would eject the ^{56}Ni amount, enough to reproduce the ^{56}Ni yield of SN 2007bi, if the central region of the progenitor has collapsed before the explosion. We expect that aspherical CC SN explosion with an ~ 40–$60\,M_\odot$ CO-core progenitor ejects ^{56}Ni, enough to reproduce the ^{56}Ni yield observed in SN 2007bi. The degree of asphericity of the explosion reproducing observational features of SN 2007bi depends on progenitor mass and explosion energy.

The elemental yields of C, N, O, Na, Mg and Ca were measured using late-time spectra in SN 2007bi (Gal-Yam et al. 2009). We show the yields of these elements for four cases of the CC SN models in this study and PI SN models in Heger & Woosley (2002) and Umeda & Nomoto (2002) in Table 3. The ranges of the measured yields in SN 2007bi are also listed.

For most elements, the yields in both the CC SN models and PI SN models are larger than the corresponding observed yields. On the other hand, the ejecta mass of SN 2007bi was estimated to be $36 < M_{ej} < 173\,M_\odot$ from the scaling relations of the rise time and the photospheric velocity (Supplementary Information of Gal-Yam et al. 2009). They suggested that a part of light elements are contained in unilluminated materials. The hidden amount of the ejecta is still quite uncertain. Therefore, we consider that it is still difficult to discuss the differences between the yields evaluated in CC SN and PI SN models and the observed yields. It is important to find the relation between the ejecta containing such a huge mass and the emitted spectra.

5.3 Ejecta velocities and rise time of light curve

The ejecta velocities of SN 2007bi were estimated by using the spectra of O, Fe, Si and Ca in 54–134 d (Young et al. 2010). The obtained ejecta velocities are 12 000–16 000 km s^{-1} for Ca II H&K lines and 10 000–12 000 km s^{-1} for Fe II. 7600–9800 km s^{-1} for Ca II near-IR, 5500–8000 km s^{-1} for Si II and 4500 km s^{-1} for the lower limit of O I.

Here, we evaluate the velocity distributions of O, Fe, Si and Ca in aspherical explosions of the collapsed 110 and $250\,M_\odot$ models. We note that the observed ejecta velocities do not indicate the bulk velocities of the ejecta. This is because the observed period is before the nebular phase and the velocities depend on the strength of absorption. Thus, it is difficult to discuss explosion features from the comparison between the observed velocities and the evaluated ones. Although we do not discuss the comparison between the observed and evaluated velocities, this evaluation will help understanding explosion features of SLSNe that will be observed in the future through the observations of the ejecta velocities in the nebular phase.

Fig. 6 shows the ejected masses of O, Fe, Si and Ca as a function of the ejecta velocity and the opening angle. Panels (a)–(d) indicate the velocity distributions of the collapsed $250\,M_\odot$ model. Most of O ejecta have a velocity of ~ 6000–$20\,000$ km s^{-1} with small opening-angle dependence. The minimum velocity and the amount of slower ejecta indicate more significant dependence on the opening angle. The minimum velocity is about 6000 km s^{-1} for spherical explosion and ~ 3000 km s^{-1} for the explosion with $\theta_{op} = 11°25$. The amount of slower O ejecta increases with decreasing opening angle of the explosion.

The velocity distribution of Fe ejecta also depends on the opening angle. The velocity range of the Fe ejecta in the spherical explosion is 1000–6500 km s^{-1}, which is narrower than O for the spherical explosion. The velocity dispersion is caused by the large ^{56}Ni production in wide spatial range of the innermost region. As the opening angle decreases, the maximum velocity becomes faster and slow ejecta increase. At the same time, the velocity dependence of the ejected amount becomes smaller. In the case of $\theta_{op} = 11°25$, the velocity range extends to 1000–13 500 km s^{-1}. Both the ejecta masses of faster and slower components increase.

The velocity dependence of Si and Ca masses moderately depends on the opening angle. The velocity range in the spherical explosion is ~ 5000–14 000 km s^{-1}. The minimum velocity decreases and slower ejecta increases with decreasing the opening angle.
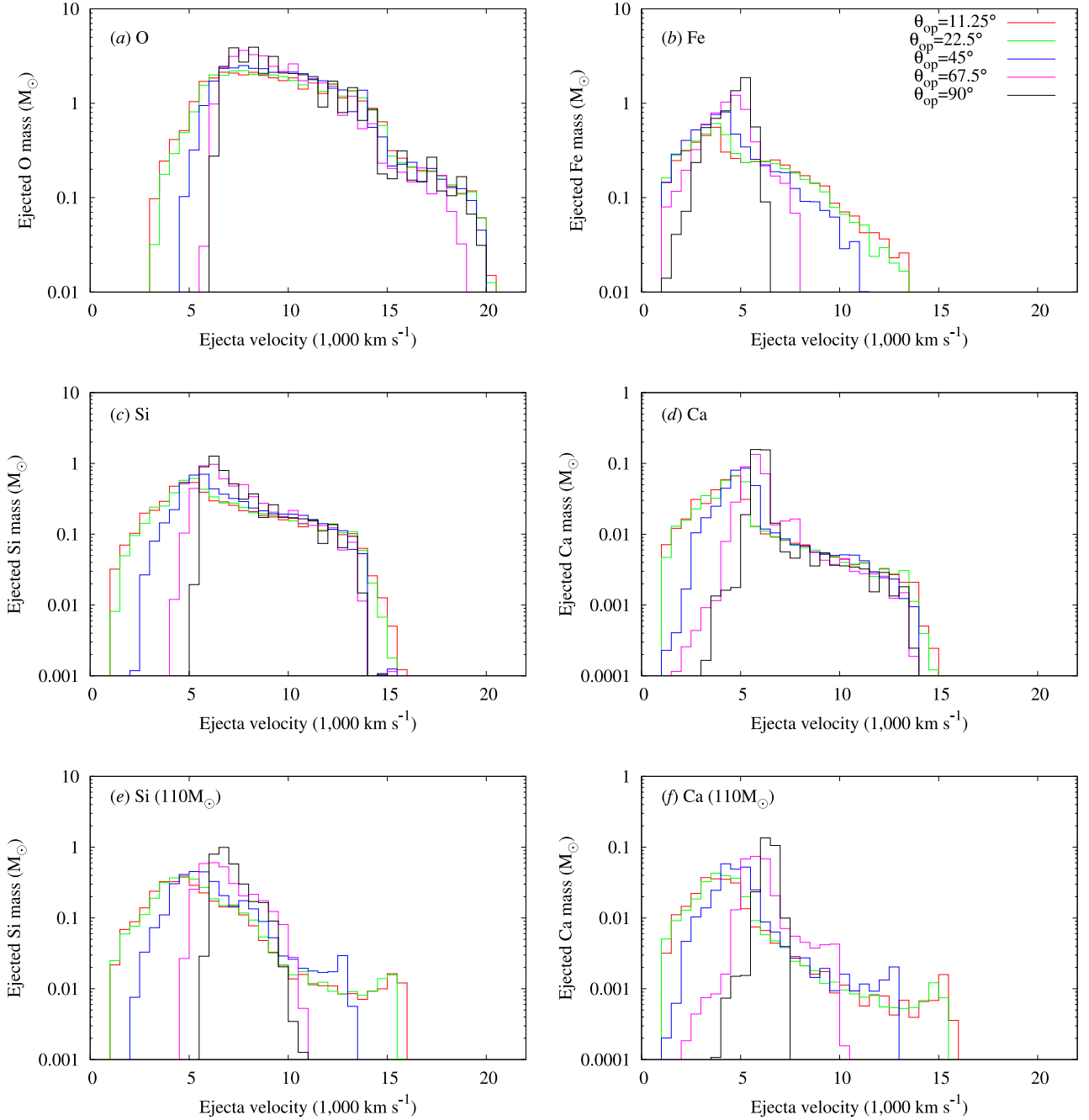
Figure 6. Velocity distributions of ejected masses of O (a), Fe (b), Si (c) and Ca (d) in aspherical explosions of the collapsed 250 M$_\odot$ model, and Si (e) and Ca (f) in the collapsed 110 M$_\odot$ model. The red, green blue, purple and black lines correspond to the cases of the opening angles of θ_{op} = 11°.25, 22°.5, 45°, 67°.5 and 90°, respectively.

We also show the velocity distributions of Si and Ca masses of the 110 M$_\odot$ model in Figs 6(e) and (f), respectively. Although the velocity range is narrow in spherical explosion, the dependence of the velocity on the opening angle is similar to the 250 M$_\odot$ model. Thus, aspherical explosions of the collapsed models produce wide velocity dispersion of SN ejecta.

We briefly discuss the velocity distributions in the uncollapsed models. When the opening angle of the explosion is small, the velocity distribution is larger than the corresponding collapsed model. In the case of the 250 M$_\odot$ model with θ_{op} = 11°.25, the O mass decreases to 1500 km s^{-1} and the Fe, Si and Ca masses increase up to

18 000 km s^{-1}. In the case of the 110 M$_\odot$ model with θ_{op} = 11°.25, the fastest component of Si and Ca is 20 000 km s^{-1}. On the other hand, the velocity distributions of the explosion models reproducing the ^{56}Ni mass of SN 2007bi are also similar to the spherical explosions of the collapsed models. These explosion models have moderate opening angles.

At last, spherical explosions indicated narrow ranges of the ejecta velocities for Fe in the 110 and 250 M$_\odot$ models, and Si and Ca in the 110 M$_\odot$ model. On the other hand, aspherical explosions indicated wider ranges of the ejecta velocities. An aspherical explosion causes wide velocity distribution of various elements even if large-scale

mixing does not occur in late time. These characteristics of the velocity distribution would constrain sphericity of SLSNe.

The rise time is a parameter characterizing the light curve of an SN. Spherical CC SN model in Moriya et al. (2010) reproduced the light curve of SN 2007bi. They evaluated the light curve assuming three cases of ejecta mixing and obtained the rise time of 52 d (full mixing), 67 d (half mixing) and 85 d (without mixing). They also reproduced the light curve by a PI SN model. The obtained rise time is $\sim$150 d. The rise time can be approximately estimated as the relation $\tau_{\rm rise} \propto (M_{\rm ej}^3/E_{\rm ex})^{1/4}$ (e.g. Nakamura et al. 2001). The rise time is roughly evaluated as $\tau_{\rm rise} \sim (7.6\text{–}12.4)(M_{\rm ej}^3/E_{\rm ex,51})^{1/4}$ d using $(M_{\rm ej}^3/E_{\rm ex,51})^{1/4} = 6.85$ for the CC explosion model in Moriya et al. (2010). Taking account of the uncertainties in the rise time and the mixing, we consider that the range of $(M_{\rm ej}^3/E_{\rm ex,51})^{1/4}$ available for the rise time of SN 2007bi is between 4.2 (short rise time and without mixing) and 11.2 (long rise time and full mixing). Here, we discuss the rise time of our SN models taking into account this dependence.

In spherical explosions, we investigated the dependence on the explosion energy. The rise time becomes shorter with increase in the explosion energy. When the explosion energy is between $E_{\rm ex,51} = 20$ and 100, where the ^{56}Ni yield of SN 2007bi is reproduced, the range of $(M_{\rm ej}^3/E_{\rm ex,51})^{1/4}$ is 5.12–7.66 and 6.74–10.1 for the 110 and 250 $M_\odot$ models, respectively. Thus, these explosion models would reproduce the light curve of SN 2007bi if ejecta mixing is appropriate.

In aspherical explosions, we investigated the dependence on the opening angle with a given explosion energy. Since the ejecta mass increases with the opening angle, the rise time also increases. The range of $(M_{\rm ej}^3/E_{\rm ex,51})^{1/4}$ is 5.77(4.63)–6.11(6.08) and 7.21(6.26)–7.37(7.36) for the collapsed (uncollapsed) 110 and 250 $M_\odot$ models. The rise time of the 250 $M_\odot$ models seems to be close to that in the CC SN model in Moriya et al. (2010). On the other hand, the rise time of jet-like explosion of the 110 $M_\odot$ models would be small. Among the explosion models reproducing the ^{56}Ni yield of SN 2007bi, the minimum value of $(M_{\rm ej}^3/E_{\rm ex,51})^{1/4}$ is 5.77 (6.08) and 7.20 (6.92) for the collapsed (uncollapsed) 110 and 250 $M_\odot$ models. Thus, we expect that spherical and aspherical CC explosion models reproducing the ^{56}Ni yield of SN 2007bi would also reproduce the light curve of SN 2007bi.

5.4 Surface He amount

In our progenitor models, a small amount, less than 1 $M_\odot$, of He remains in the outer layer. PI SN models for SN 2007bi suggested in Yusof et al. (2013) would also remain He in the envelope. The He amount hidden in an SN Ic is an unclarified problem. He lines appear through the excitation of He by non-thermal electrons induced by γ-rays from ^{56}Ni and ^{56}Co. The strength of the lines complexly depends on the amounts of He and ^{56}Ni, and other elements to thermalize electrons. The He amount hidden in 1–3 $M_\odot$ SN Ic ejecta was evaluated in Hachinger et al. (2012). The He amount hidden in more massive SNe Ic should be investigated for discussing the possibilities of SNe Ic from metal-poor very massive stars and PI SNe Ic.

5.5 Mass-loss during pulsational pair instability

A star with $M_{\rm MS} = 250 \, M_\odot$ experienced PPI during the Si burning. Although eruptive mass-loss is induced by PPI, we did not consider this effect. The mass lost during PPI for the He star models with 48–60 $M_\odot$ was investigated in (Woosley et al. 2007, see their supplementary information). They obtained that the mass of 7–18 $M_\odot$ was lost during PPI and the final mass ranges in 40–49 $M_\odot$. Chatzopoulos & Wheeler (2012b) evaluated the mass lost in one pulsation of PPI for metal-poor rotating stars. The pre-PPI SN stars with 41–58 $M_\odot$ lost the mass of 1.9–7.3 $M_\odot$. Thus, we expect that the 250 $M_\odot$ star in this study will become $\sim$40–50 $M_\odot$ after PPI. In this case, explosion feature of the SN will be similar to the SN explosion of the 110 $M_\odot$ model (43 $M_\odot$ progenitor) and aspherical explosion reproducing the ^{56}Ni yield of SN 2007bi would be possible. The above two studies also discussed the possibility that the collisions of the ejected material with the earlier ejecta during PPI induce very bright events like SLSNe. Recently, analytical light-curve models indicated that the light curve of SN 2007bi can be explained by the collision of SN ejecta with hydrogen-deficient circumstellar matter in addition to the radioactive decays of ^{56}Ni and ^{56}Co of $\sim$0.5 $M_\odot$ (Chatzopoulos et al. 2013). In this case, less energetic explosion is possible.

5.6 Prospects

We set the explosion energy of $E_{\rm ex,51} = 50$ and 70 for the 110 $M_\odot$ and 250 $M_\odot$ SN models, respectively. Such energetic explosions have been estimated through observations in SN Ic 1999as and GRB 031203/SN 2003lw (e.g. Nomoto et al. 2006). There are some possibilities of the explosion mechanism of aspherical CC SNe. One is a launch of the relativistic jet driven by magnetar formation (e.g. Takiwaki, Kotake & Sato 2009). Another is a black hole and accretion disc formation and the consequent jet production, i.e. collapsar scenario (MacFadyen & Woosley 1999). These mechanisms would have induced an aspherical energetic explosion and the explosion would have produced the ^{56}Ni yield observed in SN 2007bi.

SNe Ic associated with γ-ray bursts (GRB/SNe Ic) have been found in host galaxies having similar metallicities to the host galaxy of SN 2007bi (Young et al. 2010). GRB is a highly jet-like event and GRB/SNe Ic were observed as jet-like explosions (Maeda et al. 2008). Broad-lined SNe Ic also have been found in slightly metal-rich environments than the host galaxies of GRB/SNe Ic. Discussion of the relation between these SNe Ic and SLSNe Ic like SN 2007bi would be important for clarifying the SN events during galactic chemical evolution.

We should note that such an extreme energetic CC explosion has not been observationally ruled out, although the explosion mechanism has not been theoretically established. We showed in this study the possibility of such an extreme energetic CC explosion, enough to explain the ^{56}Ni yield of SN 2007bi within uncertainties in the mass-loss rate in very massive stars. As a significance of this study, we consider that this study will extend to future studies to clarify if such an explosion is possible or not.

There are several SLSNe expected to be the explosions from very massive stars. SN 1999as showed the light curve similar to SN 2007bi in photospheric phase (Gal-Yam 2012) and more than 4 $M_\odot$ of ^{56}Ni was estimated to be ejected (Deng et al. 2001). Recently, PTF10nmn observed by the Palomar Transient Factory and PS1-11ap found by the Panoramic Survey Telescope and Rapid Response System 1 were suggested to be candidates of PI SNe (Gal-Yam 2012, and references therein). Additional two SLSNe were also observed at redshifts $z = 2.05$ and 3.90. They are also candidates of a PI SN and a PPI SN from photometric and far-ultraviolet data (Cooke et al. 2012). Very recently, the observations of PTF12dam and PS1-11ap were reported and magnetar-energized ejecta were proposed (Nicholl et al. 2013). Although the event rate of such

SLSNe is very small, the measurements of the SLSNe, which help constraining explosion mechanism and progenitor mass of each SN, will increase in future.

6 CONCLUSIONS

We have investigated the dependence of the final mass and the fate on the MS mass and the metallicity of massive stars. We expect that very massive stars with $M_{MS} \gtrsim 100\,M_\odot$ and $0.001 < Z \lesssim 0.004$ become CC SLSNe Ic like SN 2007bi. Metal-poor stars would explode as SNe II or SNe Ib even if they explode as PI SNe. Stars with $M_{MS} \sim 110$–$150\,M_\odot$ and $Z \lesssim 0.001$ would become PPI SNe Ic if the whole H and He layer is lost during PPI. The evaluation of the He amount in SN ejecta of very massive stars to make He lines is important for determining SN types.

We also investigated the dependence of the total ejecta mass and the yields of ^{56}Ni, O and Si on the explosion energy as well as asphericity of the CC SN models with $M_{MS} = 110$ and $250\,M_\odot$ and $Z = 0.004$. In the case of spherical explosions, the yield of ^{56}Ni produced in the SN increases with the explosion energy. The SN explosion with $E_{ex,51} \gtrsim 20$ produces the ^{56}Ni amount enough to reproduce the amount observed in SN 2007bi. In the case of aspherical explosions, the total ejecta mass and the yields of ^{56}Ni, O and Si increase with the opening angle. The aspherical CC SNe of the collapsed 110 and $250\,M_\odot$ models reproduce the ^{56}Ni yield observed in SN 2007bi. In the uncollapsed progenitor models, moderately aspherical CC SNe also reproduce. These SNe indicate the velocity distribution up to $\sim 13\,000$–$15\,000$ km s^{-1} in O, Si, Ca and Fe. Therefore, an aspherical CC SN explosion evolved from a very massive star is a possibility for the explosion of SN 2007bi. The relation between SLSNe like SN 2007bi and GRB/SNe Ic and broad-lines SNe Ic would bring about new knowledge of SN events during galactic chemical evolution.

ACKNOWLEDGEMENTS

REFERENCES

Chatzopoulos E., Wheeler J. C., 2012a, ApJ, 748, 42
Chatzopoulos E., Wheeler J. C., 2012b, ApJ, 760, 154
Chatzopoulos E., Wheeler J. C., Vinko J., Horvath Z. L., Nagy A., 2013, ApJ, 773, 76
Colella P., Woodward P. R., 1984, J. Comput. Phys., 54, 174
Cooke J. et al., 2012, Nature, 491, 228
Crowther P. A., Schnurr O., Hirschi R., Yusof N., Parker R. J., Goodwin S. P., Kassim H. A., 2010, MNRAS, 408, 731
Deng J. S., Hatano K., Nakamura T., Maeda K., Nomoto K., 2001, in Inoue H., Kunieda H., eds, ASP Conf. Ser. Vol. 251, New Century of X-ray Astronomy. Astron. Soc. Pac., San Francisco, p. 2001
Gal-Yam A., 2012, Science, 337, 927
Gal-Yam A. et al., 2009, Nature, 462, 624
Hachinger S., Mazzali P. A., Taubenberger S., Hillebrandt W., Nomoto K., Sauer D. N., 2012, MNRAS, 422, 70
Heger A., Woosley S. E., 2002, ApJ, 567, 532
Hirschi R., Meynet G., Maeder A., 2004, A&A, 425, 649
Hoffman R. D., Woosley S. E., 1992, Stellar Nucleosynthesis Data, available at: http://ie.lbl.gov/astro/hw92_1.html
Horowitz C. J., 2002, Phys. Rev. D, 65, 043001
Langer N., Norman C. A., de Koter A., Vink J. S., Cantiello M., Yoon S.-C., 2007, A&A, 475, L19
MacFadyen A. I, Woosley S. E., 1999, ApJ, 524, 262
Maeda K. et al., 2008, Science, 319, 1220
Moriya T., Tominaga N., Tanaka M., Maeda K., Nomoto K., 2010, ApJ, 717, L83
Nakamura T., Umeda H., Iwamoto K., Nomoto K., Hashimoto M., Hix W. R., Thielemann F.-K., 2001, ApJ, 555, 880
Nicholl M. et al., 2013, Nature, 502, 346
Nomoto K., Tominaga N., Umeda H., Kobayashi C., Maeda K., 2006, Nucl. Phys. A, 777, 424
Okita S., Umeda H., Yoshida T., 2012, in Kubono S., Hayakawa T., Kajino T., Miyatake H., Motobayashi T., Nomoto K., eds, AIP Conf. Ser. Vol. 1484, Origin of Matter and Evolution of Galaxies 2011. Am. Inst. Phys., New York, p. 418
Quimby R. M. et al., 2011, Nature, 474, 487
Sugimoto D., Nomoto K., Eriguchi N., 1981, Prog. Theor. Phys. Suppl., 70, 115
Suzuki T., Honma M., Higashiyama K., Yoshida T., Kajino T., Otsuka T., Umeda H., Nomoto K., 2009, Phys. Rev. C, 79, 061603
Takiwaki T., Kotake K., Sato K., 2009, ApJ, 691, 1360
Tominaga N., 2009, ApJ, 690, 526
Tominaga N., Maeda K., Umeda H., Nomoto K., Tanaka M., Iwamoto N., Suzuki T., Mazzali P. A., 2007, ApJ, 657, L77
Umeda H., Nomoto K., 2002, ApJ, 565, 385
Umeda H., Nomoto K., 2005, ApJ, 619, 427
Umeda H., Nomoto K., 2008, ApJ, 673, 1014
Umeda H., Yoshida T., Takahashi K., 2012, Prog. Theor. Exp. Phys., 01, A302
Waldman R., 2008, ApJ, 685, 1103
Woosley S. E., Blinnikov S., Heger A., 2007, Nature, 450, 390
Yoon S.-C., Woosley S. E., Langer N., 2010, ApJ, 725, 940
Yoshida T., Umeda H., 2011, MNRAS, 412, L78 (YU11)
Yoshida T., Umeda H., Nomoto K., 2008, ApJ, 672, 1043
Yoshida T., Suzuki T., Chiba S., Kajino T., Yokomakura H., Kimura K., Takamura A., Hartmann D. H., 2008, ApJ, 686, 448
Young D. R. et al., 2010, A&A, 512, A70
Yungelson L. R., van den Heuvel E. P. J., Vink J. S., Portegies Z. S. F., de Koter A., 2008, A&A, 477, 223
Yusof N. et al., 2013, MNRAS, 433, 1114

This paper has been typeset from a TEX/LATEX file prepared by the author.